JOURNAL OF Applied Polymer SCIENCE

Optimal Performances of Ultrasound Treated Kenaf Fiber Reinforced Recycled Polypropylene Composites as Demonstrated by Response Surface Method

M. R. Islam, M. D. H. Beg, A. Gupta, M. F. Mina
Faculty of Chemical and Natural Resources Engineering, Universiti Malaysia Pahang, Gambang-26300, Kuantan, Malaysia
Correspondence to: M. D. H. Beg (E-mail: dhbeg@yahoo.com)

ABSTRACT: Kenaf fiber (KF) reinforced recycled polypropylene (RPP) composites were produced by melt cast method. To improve interfacial adhesion between fiber and RPP matrix, fiber surface modification was carried out by means of ultrasound treatment. Maleic anhydride grafted polypropylene (MAPP) was used as a coupling agent. Composites were examined by mechanical test, melt flow indexing test, scanning electron microscopy, thermogravimetric analysis (TGA), and differential scanning calorimetry (DSC). Water uptake analysis and accelerated weathering test were carried out to find the suitability of the composites in outdoor application. Among the raw fiber contents ranging 10−50 wt % in the composites, the maximum tensile strength (TS) was observed at 40 wt % KF loading without using MAPP. Treated KF-based composite with MAPP promotes this maximum TS value, which is 57% higher than that of raw KF-based composite. TGA and DSC analyses exhibit an enhancement of thermal stability in treated KF-reinforced RPP composites with MAPP. Incorporation of MAPP in the composites shows higher activation energy, suggesting improved interfacial bonding between fibers and matrix. Response surface method was employed to demonstrate the optimal treatment parameters for TS, showing excellent agreement with the observed values. © 2012 Wiley Periodicals, Inc. J. Appl. Polym. Sci. 000: 000–000, 2012

KEYWORDS: recycling; composites; thermogravimetric analysis (TGA); degradation; fibers

Received 9 June 2012; accepted 8 August 2012; published online
DOI: 10.1002/app.38454

INTRODUCTION

Natural fibers have received considerable attention as an environmentally friendly alternative to inorganic fibers in order to expand the application areas of engineering composites.[1,2] Despite their ecological advantages like renewability, incineration, harmlessness, and low manufacturing cost over synthetic counterparts, natural fibers possess two major disadvantages, such as moisture absorption and incompatibility to polymer matrix, which deteriorate both mechanical and thermal properties of the resulting composites.

Lignocellulosic fibers contain polarized hydroxyl groups, which are prone to form hydrogen bonds among fibers, resulting in the fibers agglomeration during composite fabrication. The process of agglomeration makes uneven dispersion and poor adhesion of fibers in the polymer matrix and ultimately weakens the composites' mechanical properties. The mechanical performances of the composites decline because of the discontinuous stress transfer from matrix to fibers. To overcome this drawback, modification of fiber surface has been reported, and an improved interfacial adhesion between fiber and matrix has been established.[3] Alkali treatment method has been extensively followed to improve the fiber–matrix adhesion, because removal of natural and artificial impurities from the fiber develops surface roughness or sources of mechanical interlocking.[4–8] Besides, the use of coupling agent like maleic anhydride grafted polypropylene (PP) to enhance the fiber–matrix intertwining is also notable.[9]

However, chemical treatments of fiber and incorporation of coupling agents in the fabrication of fibers-reinforced composites are widely adopted traditional methods, where the former one is much time-consuming and the later one is comparatively expensive. Therefore, economically viable alternative approach has been searched for and accordingly ultrasound (ULS) treatment has emerged as a relatively new and potential route to modify natural fiber surface. ULS can develop bubbles in a liquid medium by physical process. Sudden and explosive collapse of these bubbles can generate hotspots, i.e., localized high temperature and high pressure shock waves and severe shear force that are capable of breaking chemical bonds.[10] Although ULS has been potentially used in treating some fibers,[11,12] its successful utilization in kenaf fiber treatment has not yet been reported, especially in the optimization of fiber treatment conditions. On the other hand, response surface method (RSM) is a statistical

technique, which explores the relationship between several explanatory variables and one or more response variables, where the main idea of RSM is to use a sequence of designed experiments to obtain an optimal response.[13] The RSM is basically used in central composite design, one-factor design, and D-optimal design and has been successfully proven to be an effective method for optimization of biomass treatment.[13]

It is worthwhile to note that the extensively used thermoplastics like polyethylene (PE), polyethylene terephthalate (PET), polyvinyl chloride (PVC), and PP render harmful ecological impact when they are released as wastages. To protect the environment from danger, recycled PET, PE, PVC, etc. plastics have been used as interesting research materials in composites fabrication. Previous investigations suggests that no considerable reduction of tensile strength and tensile modulus were observed for recycled PET and PE, whereas an improved mechanical performance was obtained for PE with the inclusion of coupling agents.[14,15] Concerning clean ecology, we are motivated to use recycled PP for producing value-added new products. Since kenaf fiber is abundantly produced in Malaysia and available at low price, its use as reinforcements in the recycled PP can not only give rise to cost-effective new composite materials but also increase its recycling rate, which is now 5% in this country. Although, ULS treatment is now being popularly used, a particular emphasis has been given in this article to treat kenaf fibers by means of RSM to abstract their optimal performances. Further points of interest in this work are to observe the effects of fiber treatments by ULS on physical, mechanical, morphological, and thermal properties of recycled PP composites prepared from differently loaded fibers with and without coupling agents and to confirm the optimal condition by RSM.

EXPERIMENTAL

Materials

Raw kenaf fibers (RKFs) were collected from Kampung Merchong, Pahang, Malaysia. Recycled PP of commercial name PP black copo was supplied by Efficient Growth Sdn Bhd, Selangor, Malaysia. Maleic anhydride grafted polypropylene (MAPP) of trade name Polybond 3200 was a coupling agent, supplied by MTBE (M) Sdn Bhd, Gebeng, Kuantan, Malaysia.

Sample Preparation

Fiber Treatment by Ultrasound. ULA cleaner, model-DAI-HAN-DH.D 300H having HF-Frequency up to 40 kHz, sonication power range from 0 to 100%, tank capacity of 3 L, and temperature range from ambient condition to 100°C was used to treat KF in the water medium, where temperature of water and sonication power of ULS were considered as treatment variables. Firstly, three different types of treated KFs were prepared at 60°C by ULS using different sonication powers such as 50, 75, and 100%. Secondly, three types of ULS treated KFs (UKFs) were obtained at temperatures of 60, 80, and 95°C using merely the high sonication power. In each case, the sonication time was 1 h.

Preparation of Composites. Air-dried RKFs were shredded into small size by a plastic crusher. These shredded fibers of length 2–5 mm and diameter 0.05–0.08 mm, having the average aspect ratio of 54, were dried at 70°C in an oven to remove the moisture content. RKFs were compounded with recycled polypropylene (RPP) by means of a Prism Eurolab 16 twin-screw extruder having $L/D = 40$ (length/diameter of the screw), rotational screw speed of 125 per min, and barrel temperature range of 170–190°C from the feeding zone to the die zone, respectively. Extrusion of RKFs and RPP were performed with the fiber contents of 10, 20, 30, 40, and 50 wt %, and samples for tensile test were prepared by an injection molding machine (NESSEI, model-PNX60) at 190°C. Tensile properties were measured for optimization of the fiber content in the composites. Tensile properties were also observed for the UKFs-reinforced RPP composites in order to optimize the ULS treatment and temperature. The treated fibers used had the length 0f 2–5 mm and diameter 0.04–0.06 mm, having the average aspect ratio of 70. The optimized simultaneous ULS and temperature-treated KFs are referred here-in-after to OUKFs. Then, MAPP was introduced in RPP and OUKFs for extrusion, keeping the coupling agent to fiber ratio of 1 : 10. The extrudates were then chopped and fed into the injection molding machine for preparing the test samples. The samples characterized by the following various methods were RPP, RPP/RKF composites (RKPC), MAPP loaded RKPC (MRKPC), and MAPP incorporated OUKF/RPP composites (MOUKPC).

Characterizing Techniques

Fourier Transformed Infrared Analysis. Functional group of fibers before and after ULS treatment were analyzed by a Fourier transform infrared (FTIR) spectrophotometer (model: THERMO) using the standard KBr pellet technique. Each spectrum was recorded in the wavenumber range from 4000–500 cm^{-1}.

Density Measurements. A gas pycnometer (model-micromeritics, AccuPyc II 1340) was used to determine the volume of the materials in order to calculate the density of the materials under inert helium gas. Five replicates were considered for each category of samples and average value was taken.

Melt Flow Index Measurements. The melt flow index (MFI) was determined by using a MFI tester (Dynisco Instrument) at 230°C with a standard weight of 2.16 kg. Three replicates were considered for each category of samples and average value was taken.

Tensile Test. The mechanical measurements of KF were carried out by a tensile tester, model-DIA-STRON LTD/UK (FDAS 765). Single strain fiber was taken after preparing the sample. Then crimping was done by means of a crimper. After that, sample was placed at Laser Scan Micrometer (LSM 500)-Mitutoyo to analyze the fiber dimension. Tensile tester was benched at the top and the maximum force was set at 500 N before loading the sample.

On the other hand, the tensile tests of composites were carried out according to ASTM D638-Type I using a SHIMADZU (MODEL AG-1) universal testing machine with a load of 5 kN at a crosshead speed of 10 mm/min and with a gauge length of 65 mm.

Flexural Test. The flexural test was conducted according to ASTM D790-97 standard using the same apparatus as that used

Table I. Proposed Set of Parameters Using the Central Composite Design Software

Standard	Run	Block	Factor 1 Sonication power (%)	Factor 2 Temperature (°C)	Response 1 TS (MPa)
12	1	Block1	75.00	77.50	
6	2	Block1	100.00	77.50	
9	3	Block1	75.00	77.50	
4	4	Block1	100.00	95.00	
5	5	Block1	39.64	77.50	
13	6	Block1	75.00	77.50	
3	7	Block1	50.00	95.00	
7	8	Block1	75.00	52.75	
8	9	Block1	75.00	95.00	
10	10	Block1	75.00	77.50	
11	11	Block1	75.00	77.50	
1	12	Block1	50.00	60.00	
2	13	Block1	100.00	60.00	

for the tensile test with a static load of 1 kN. The support spans were set at 50 mm, and the crosshead speed was fixed at 10 mm/min.

Impact Test. Impact strength (IS) was measured by the Charpy impact test, according to ASTM D256 with the help of an impact pendulum tester (model-ZWICK/ROELL) at a swing-angle of 90° with a hammer load of 1 J.

Thermogravimetric Measurements. Thermogravimetric measurements were carried out using a thermogravimetric analyzer (TA instrument, TGA Q500). Each sample was weighed and heated at the scanning temperature range of 25–600°C with a heating rate of 20 °C/min. Thermogravimetric analysis (TGA) was conducted in a platinum crucible under nitrogen atmosphere at a flow rate of 40 mL/min to avoid unwanted oxidation. Kinetic parameters in the thermal degradation were determined from the TGA data using the following eq. (1), given by Broido:[16]

$$\ln\left(\ln\frac{1}{y}\right) = -\frac{E_a}{RT} + \ln\left(\frac{RZ}{E_a\beta}T^2_{(d\max)}\right) \quad (1)$$

where, y = fraction of non-volatilized material not yet decomposed, $T_{d\max}$ = temperature of maximum reaction rate (°C), β = heating rate (°C/min), Z = frequency factor, E_a = activation energy (J/mol), R = gas constant (8.314 J/mol K). From the TGA data, $\ln\ln(1/y)$ versus $1/T$ plots were drawn, and from the slope of each line, the value of E_a for each sample was evaluated.

Differential Scanning Calorimetry. A thermal analyzer (TA instrument, Q-1000) was used to perform differential scanning calorimetry (DSC) of the samples in the aluminum pan with a heating rate of 20 °C/min. A heat/cool/heat method was applied using a temperature range of 25–250°C. The percentage of crystallinity (X_c) and the melting point of the samples were calculated by using an appropriate software.

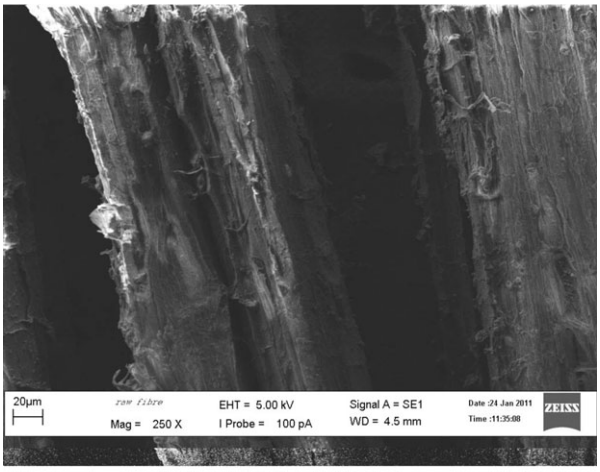

(a)

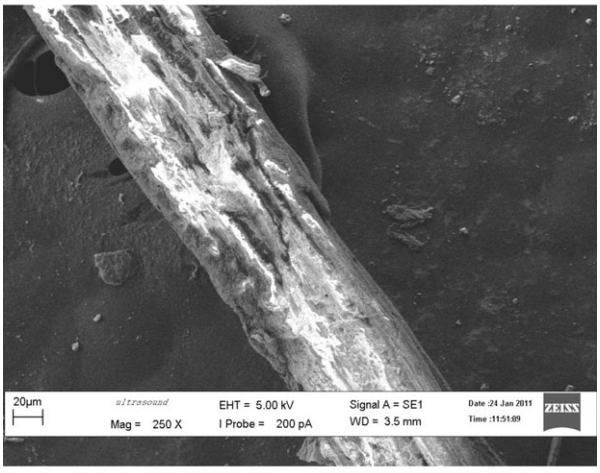

(b)

Figure 1. SEM micrographs of (a) RKF and (b) OUKF at 250× magnification.

Applied Polymer SCIENCE

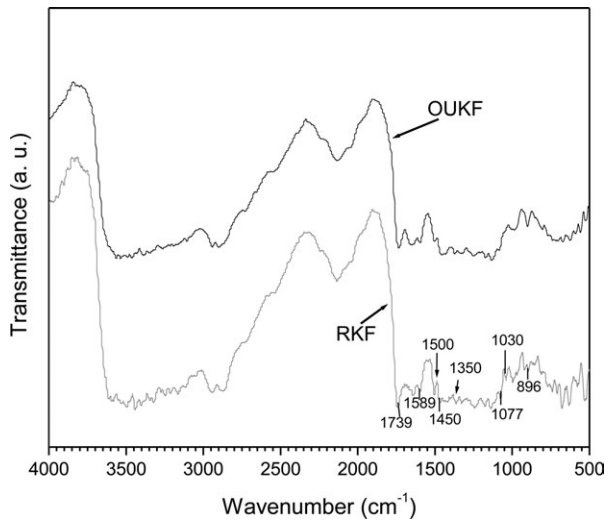

Figure 2. FTIR spectra of RKF and OUKF in the wavenumber range 4000–500 cm^{-1}.

Scanning Electron Microscopy. The surface morphologies of RKF and OUKF were monitored by a scanning electron microscope (SEM) (model-ZEISS, EVO 50), and that of composites were examined by field emission scanning electron microscopy (FE-SEM) (model-JEOL, JSM-7800F). For this purpose, samples were placed onto a metal-based holder with the help of double sided sticky carbon tape. Prior to observations, samples were coated with gold for fibers and platinum for composites by means of a vacuum sputter-coater for ease of conduction.

Water Uptake. Tensile specimens were immersed in distilled water at room temperature for various periods of time to study the moisture absorption. Then, they were taken out from water periodically and weighed. This process was continued for 150 days. The percentage of water uptake, WU (%), at time t, was calculated from eq. (2):

$$\mathrm{WU}(\%) = \frac{w_f - w_i}{w_i} \times 100 \qquad (2)$$

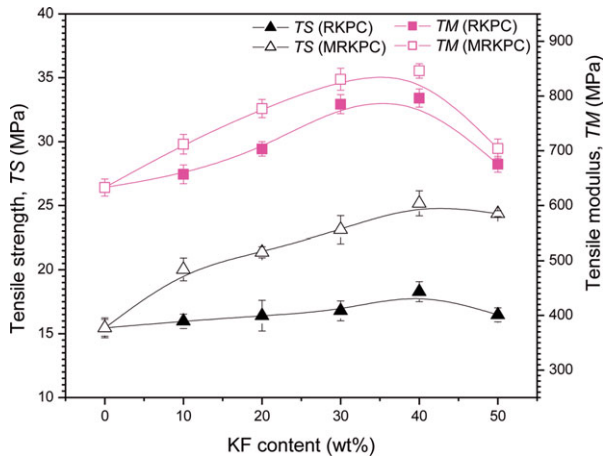

Figure 3. Tensile strength and tensile modulus of RPP, RKPC, and MRKPC. [Color figure can be viewed in the online issue, which is available at wileyonlinelibrary.com.]

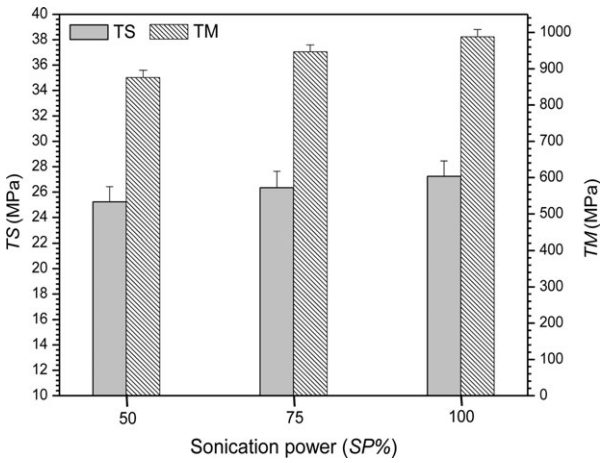

Figure 4. Tensile-strength and tensile modulus of the composites with KFs (40 wt %) treated at various sonication frequencies at 60°C.

where, w_i and w_f are the initial and final weights of the sample before immersing in water and after taking out of water, respectively. Tensile tests of the samples after water absorption were also performed.

Accelerated Weathering. Accelerated weathering tests on tensile specimens were carried out according to ASTM-G154 using an accelerated weathering tester (model-QUV/spray with solar eye irradiance control) with two cycles, namely exposition by the ultraviolet (UV) ray at 60°C and condensation for 4 h each. The UV light was exposed to the selected tensile specimens for time periods of 600, 1200, and 1800 h and their tensile measurements were carried out of the samples.

Response Surface Studies. Performance optimization of the samples in terms of fiber treatment parameters was carried out by means of Design Expert Software (DES), Version 8.0.6 Stat-Ease Inc., USA. For this purpose, sonication powers (SP %) and treatment temperature (T) were taken as the only two different variables to have the response in terms of tensile strength (TS). When a range of experimental values T = 60–95°C and SP =

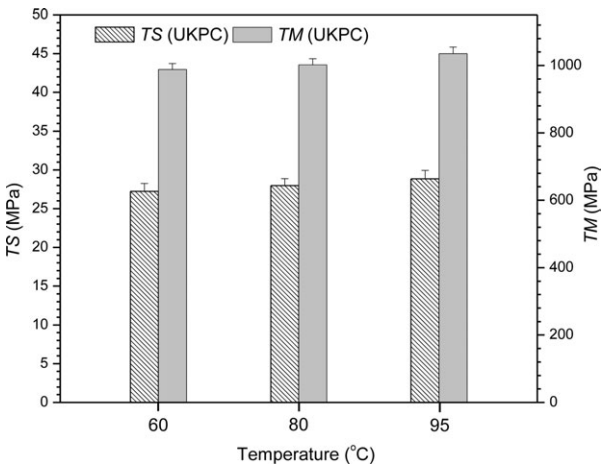

Figure 5. Tensile strength and tensile modulus of composites prepared with KFs (40 wt %) at various temperatures with 100% SP.

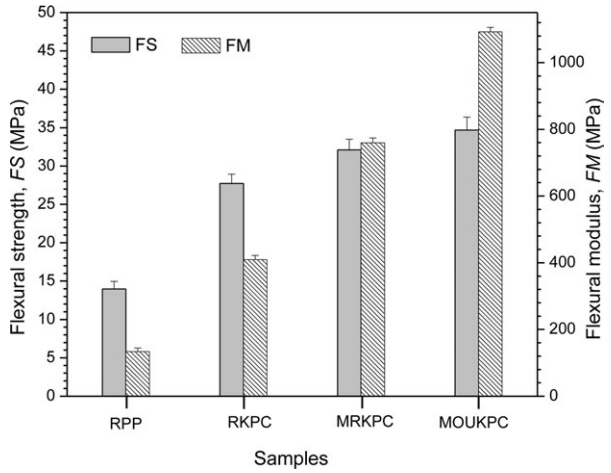

Figure 6. Flexural strength and flexural modulus of RPP, RKPC, MRKPC, and MOUKPC with 40 wt % KFs.

50–100% were used in the DES, it predicted a combination of SP% and *T* values (Table I) with which RKFs were again treated to fabricate a series of composites using these fibers. Then, the TS values of these composites were again measured and introduced into DES for getting a further set of predicted refined parameters. From the TS values corresponding to this refined set of SP% and *T*, the optimal performance parameters were validated. Using these statistical values, various graphs were plotted with the help of the DES to demonstrate the optimal performances.

Table II. Density, MFI, and IS Values of the Various Samples

Formulation	Density (g/cm^3)	MFI (g/10 min)	IS (J/m^2)
RPP	0.91	5.58	33.97
RKPCP	1.07	0.40	21.79
MRKPC	1.12	0.33	22.51
MOUKPC	1.13	0.37	27.38

RESULTS AND DISCUSSION

Surface Morphology

The surface morphologies of RKF and OUKF is presented in Figure 1, where the surface of RKF [Figure 1(a)] is observed to be comparatively smoother than that of OUKF [Figure 1(b)], suggesting that cellulose is held tightly with binding components like lignin, pectin, etc. In contrast, OUKF surface structure shows a relatively thinner diameter than RKF with fibrils and huge pores, indicating removal of debris and non-cellulosic components from the fiber. Treated fiber surface has been reportedly attributed to the removal of lignin and hemicellulose.[17]

FTIR Analysis

The FTIR spectra for RKF and OUKF are shown in Figure 2, which shows nearly similar absorption peaks for them except some variations. The important differences found between these two spectra are numbered in the range 800–1740 cm^{-1}. For RKF, the β-glucosidic linkage between sugar units of hemicelluloses appears at a wavenumber 896 cm^{-1}, and the C—O

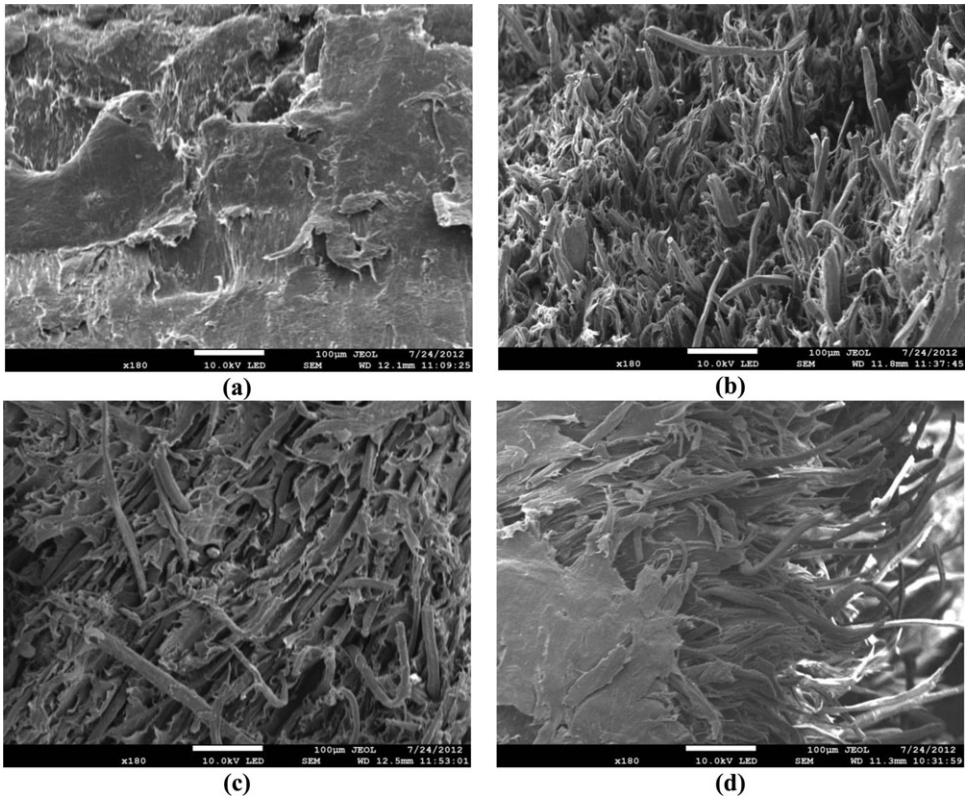

Figure 7. FE-SEM micrographs of the fractured surface for (a) RPP, (b) RKPC, (c) MRKPC and (d) MOUKPC.

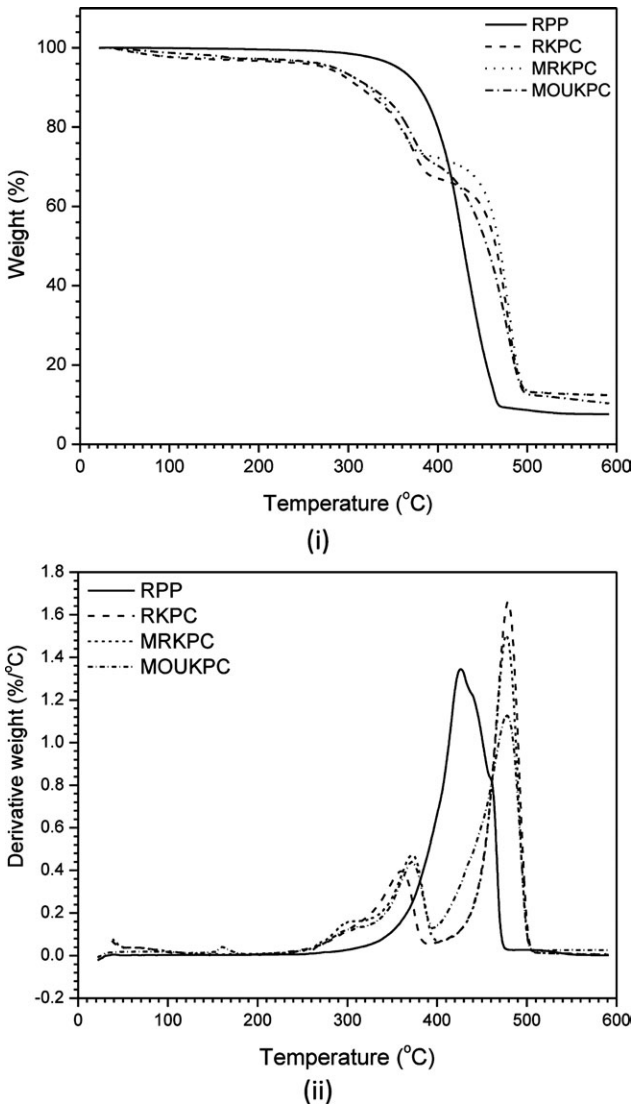

Figure 8. TGA thermograms of RPP and various composites.

stretching and O—H deformation vibrations, respectively, appearing at 1077 and 1030 cm^{-1} are characteristics of cellulose and lignin. The peaks at 1589, 1500, and 1440 cm^{-1} in the RKF spectrum are due to benzene ring stretching and CH_2 deformation of lignin, respectively. A reduction in intensities of all the above mentioned absorption peaks as well as the missing of some observed peaks of RKF in the spectrum of OUKF strongly indicates the complete or partial removal of cementing components from RKF by ULS treatment.

Furthermore, the broad intensified absorbance peak of RKF at the range 3200–3600 cm^{-1}, which represents O—H stretching of hydrogen bond, also becomes weak for the case of OUKF due to ULS treatment. Such a drop of intensity was attributed to the reduction of hydrogen linkages of removed components that were linked with cellulose and hemicellulose molecules.[18] A slight decrease in intensity in the spectrum of OUKF as compared to the intensity of RKF is found for the absorbance peaks at 1739 cm^{-1} corresponding to the C=O bonds in carboxyl and ester groups. The absorbance bands at 1450 cm^{-1} and 1350 cm^{-1} assigned to CH_3 asymmetric and —C—H symmetric deformations of lignin are also weakened due to treatment indicating lignin removal. All these results strongly suggest partial removal of hemicellulose and fatty acid due to ULS treatment and comply with reported results.[19]

Mechanical Properties

Tensile properties, such as tensile strength (TS) and tensile modulus (TM), of RKPC and MRKPC as a function of KF contents are presented in Figure 3. The observed TS value for RPP is 15.46 MPa and after inclusion of RKF, the TS of the composites are found to increase. The maximum TS and TM values are obtained at 40 wt % KF content for the samples prepared both with and without MAPP. The mechanical properties decrease when KF $>$ 40 wt %. This decrease can be attributed to the poor dispersion and agglomeration of the fibers at higher loading, as noted elsewhere.[20] The maximum TS values obtained for RKPC and MKPC are 18.3 and 25.2 MPa, respectively. Therefore, the TS increase of RKPC is $\sim$ 18% with respect to RPP and that of MKPC is $\sim$ 37% with regard to RKPC at 40 wt % RKFs loading, respectively. On the other hand, the change of TM is similar to that of TS. The values of TM are found to be 822 MPa for RKPC and 846 MPa for MRKPC. Analysis shows that the increase of TM of MRKPC from RKPC is 6% at 40 wt % RKFs loading.

Figure 4 illustrates the change of TS and TM of composites prepared with fibers which were treated with different sonication power. Evidently, high energy sonication treatment exhibits the highest TS (27.25 MPa) and TM (988 MPa) values of the composites. Figure 5 represents the TS and TM values of composites, which were prepared with KFs treated at various temperatures. Clearly, the maximum tensile properties (TS = 28.84 and TM = 1035 MPa) is observed for KFs treated at 95°C. Therefore, KFs treated at high ULS energy (SP = 100%) and at 95°C are considered as the optimized fibers which are then used for fabrication of composites with MAPP.

Figure 6 demonstrates flexural strength and modulus of RPP of various composites. It is clear that composites with coupling agent exhibit better mechanical performances. The flexural strength (FS) and flexural modulus (FM) values of MOUKPC are, respectively, found to be 34.7 and 1092 MPa, showing the maximum values among the investigated composites. Thus, the

Table III. The Values of T_d, E_a, and Amount of Residues for Various Samples, Observed by TG

Samples	Stage	T_d-range (°C)	$T_{d(max)}$ (°C)	E_a (KJ/mol)	Residue (wt %)
RPP	–	267-472	420	99.41	7.58
RKPC	1st	221-391	365	44.37	12.34
	2nd	392-501	473	67.44	
MRKPC	1st	247-381	351	50.90	12.43
	2nd	406-502	477	78.84	
MOUKPC	1st	234-312	310	49.36	10.29
	2nd	312-401	374	91.05	

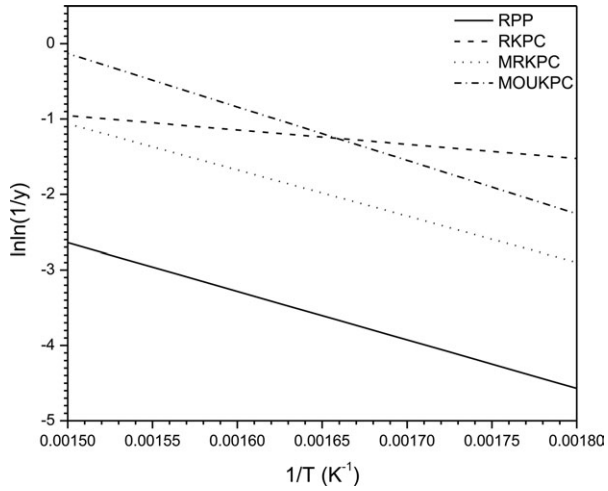

Figure 9. lnln (1/y) vs. 1/T curves for RPP and various composites.

FS increase of MOUKPC from MRKPC and RKPC is 8 and 15% and the FM increase is 43 and 85%, respectively. Incorporation of fiber usually increases the stiffness of the resultant composites, but ULS treatment of fiber as well as the inclusion of coupling agents improves the mechanical properties of the resulting composites considerably.

On the other hand, the values of IS for various samples are presented in Table II. The IS decreases with fiber loading due to weak interfacial bonding between fiber. Although, incorporation of fiber lowers the IS by ~ 38%, the IS value of MOUKPC increases by ~ 5.7% from RKPC. This was reportedly for the removal of lignin and the use of coupling agent in composites.[20]

Density and MFI Analyses

The measured values of density and MFI for various samples are included in Table II. The order of observed density values for the samples can be arranged as MOUKPC>MRKPC>RKPC>RPP. Since, the density of RKF (1.50 g/cm^3) is higher than that of RPP (0.91 g/cm^3), the larger density observed for RKPC than RPP is rational. Katsoulotos et al. reported similar observation in case of linear low density PE-cellulosic fiber composites.[21] The increased density MOUKPC indicates a better interfacial adhesion between fiber and recycled PP matrix as compared to MRKPC. In contrast, the measured MFI values of the samples follow the order: MOUKPC<MRKPC<RKPC<RPP. The reduction in flow property for MOUKPC is probably due to the consequence of the removal of cementing components from KFs by treatment as well as the presence of MAPP.

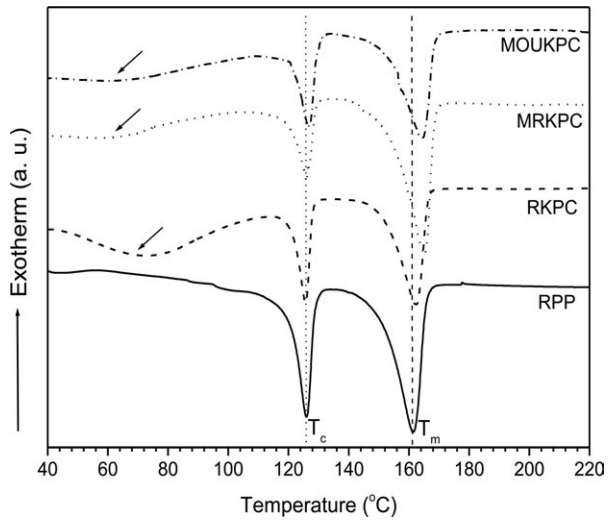

Figure 10. DSC thermograms for RPP and various composite materials.

Table IV. The Values of T_c, T_m, ΔE, and X_c of the Samples Obtained from DSC Analysis

Samples	T_c (°C)	T_m (°C)	ΔE (J/g)	X_c (%)
RPP	125.5	164.25	27.48	21.9
RKPC	125.7	163.13	30.14	24.0
MRKPC	126.4	163.80	39.16	31.2
MOUKPC	126.8	163.23	48.25	38.5

Surface Morphology of the Composites

FE-SEM micrographs of the fractured surfaces of various samples are presented in Figure 7. While the micrograph of RPP shows uneven matrix, those of composites show similar nature with random distribution of fibers. For instance, while huge fibers are pulled out from RKPC after stretching, no noticeable fibers come out from both MRKPC and MOUKPC. Comparison of the morphology from the micrographs of MRKPC and MOUKPC, the later one shows less fiber detachment from the matrix. This examination clearly reveals poor interfacial bonding between KFs and RPP in RKPC and this interfacial adhesion is enhanced by both fiber treatment and incorporation of coupling agent, as demonstrated by SEM images of MRKPC and MOUKPC. As a result of the increase of fiber-surface roughness by treatment, adhesion between fiber and matrix were improved, and the addition of MAPP strengthens this adhesion more substantially. This fact can be verified from micrographs of

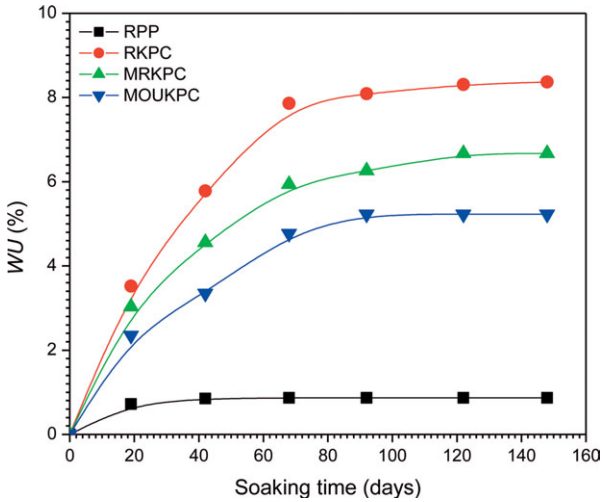

Figure 11. Water-uptake (%) versus soaking time (days) plots for RPP and various composites. [Color figure can be viewed in the online issue, which is available at wileyonlinelibrary.com.]

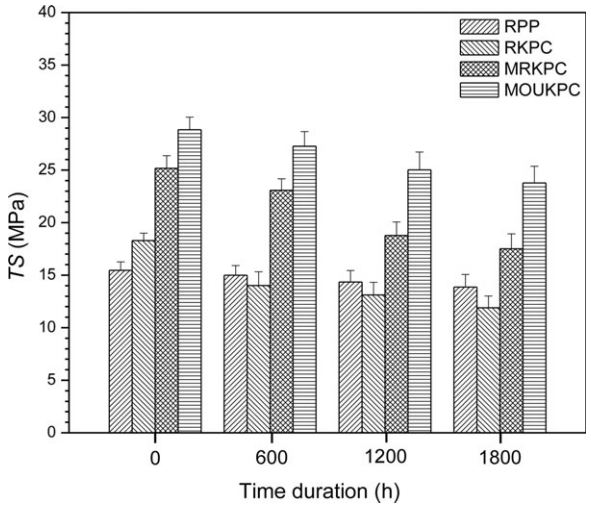

Figure 12. TS of RPP and various composites before and after accelerated weathering.

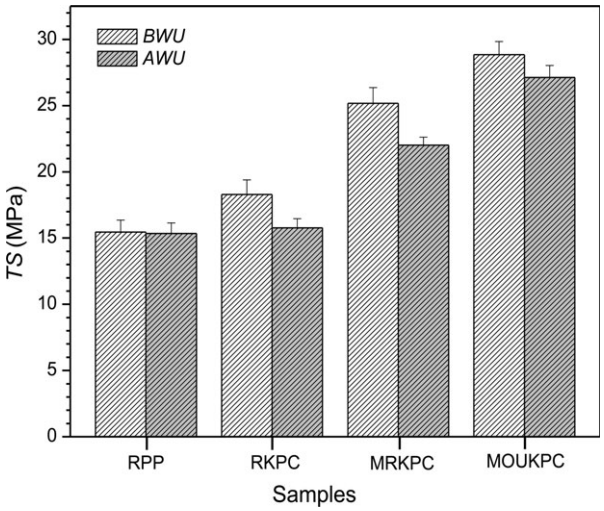

Figure 13. TS of RPP and various composites before (BWU) and after water uptake (AWU).

MOUKPC, where fiber pull-out is less visible. These results support the improved mechanical performances of the composites.

Thermal Analysis

The TGA thermograms of various samples are shown Figure 8(i), indicating the weight fall or the degradation of the samples at one-stage in RPP and two-stages in the composites. This difference of degradation in the samples is due to the presence of fibers. The range of degradation temperature (T_d) and the temperature of maximum degradation ($T_{d(\max)}$) are tabulated (Table III). Obviously, the weight loss commences at higher temperatures, known as the onset temperature of thermal degradation. The onset temperatures for RKPC, MRKPC, and MOUKPC are 268, 293, and 294°C, respectively. These results clarify that the thermal degradation in MOUKPC occurs relatively at a higher temperature. The derivative of TG (DTG) thermograms are shown in Figure 8(ii), which indicates the 1st degradation peak for RKPC, MRKPC, and MOUKPC at 359, 372.5, 373°C, respectively. However, activation energy, E_a has been calculated using Broido's plots (Figure 9) for all samples in order to understand the thermal degradation mechanism. The values of E_a are also introduced in Table III. The E_a is known to represent the energy barrier preventing polymer molecules to move from one location to the other. Thus, the higher value of E_a represents more thermal stability of a sample. The observed results thus strongly demonstrate that MOUPC is thermally more stable as compared to other composites. Similar results are reported in the literature.[22]

The DSC thermograms of the samples are presented in Figure 10. The two endothermic peaks for RPP observed at $\sim$ 125°C and $\sim$ 164°C correspond to its crystallization and melting temperatures (T_c and T_m),[22] respectively. An additional peak appears at 80°C (indicated by arrows) in case of

Table V. The Observed TS Values of the Composites Prepared from Suggested Parameters by RSM

Std	Run	Block	Factor 1 A: Sonication power (%)	Factor 2 B: Temperature (°C)	Response 1 TS (MPa)
12	1	Block1	75.00	77.50	26.56
6	2	Block1	100.00	77.50	27.98
9	3	Block1	75.00	77.50	26.21
4	4	Block1	100.00	95.00	28.84
5	5	Block1	39.64	77.50	25.11
13	6	Block1	75.00	77.50	26.44
3	7	Block1	50.00	95.00	26.97
7	8	Block1	75.00	52.75	26.01
8	9	Block1	75.00	95.00	27.35
10	10	Block1	75.00	77.50	26.01
11	11	Block1	75.00	77.50	25.92
1	12	Block1	50.00	60.00	25.23
2	13	Block1	100.00	60.00	27.25

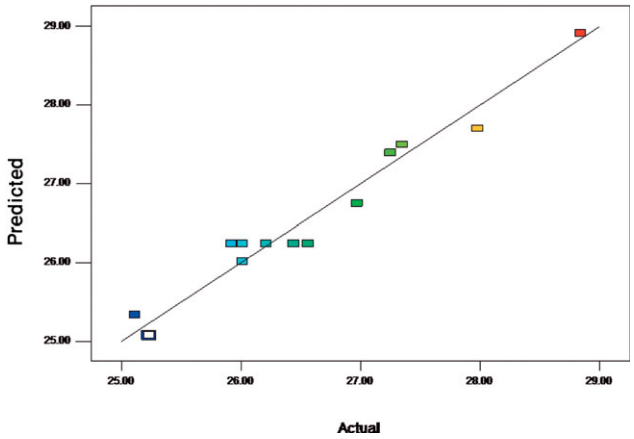

Figure 14. Predicted versus actual (experimental) value of the response. [Color figure can be viewed in the online issue, which is available at wileyonlinelibrary.com.]

composites due to the release of water molecules from KFs. After incorporation of KFs in RPP, the peak position of T_c does not change conspicuously but that of T_m is shifted to higher temperature. The observed values of T_c, T_m, and enthalpy (ΔE_m) calculated from the melting transition are inserted in Table IV. Considering $\Delta E_m = 209$ J/g for the 100% crystalline PP,[23] analysis shows that the X_c value for RPP is the lowest and that for MOUKPC is the highest, giving rise to a gradual increase. Similar results were reported by Qin et al., who showed an increase of crystallinity from 10.7 to 16.6% for rice-straw fiber modified by poly(butyl acrylate) in the polylactic acid.[24] Incorporated KFs may act as nucleating agent, which ultimately increases the crystallinity of composites. Crystallinity increases due to treated fiber in the presence of coupling agent, because strong interaction between fiber and matrix provides transcrystallinity effect, which was found by Marcovich and Villar for the case of linear low density PE composite with wood flour.[25]

Water Absorption

The WU of the samples at various samples is displayed in Figure 11. The dependence of WU on time for all samples is similar except that the amount of WU at a particular time is different for different samples. Generally, PP is hydrophobic in nature, but a lower WU value in RPP is supposed to be due to the presence of very small amount of inorganic fillers and microvoids. Evidently, the WU% of the samples follows the order RKPC>MRKPC>MOUKPC. This suggests that less reactive groups, which have affinity to absorb water, are present in MRKPC and MOUKPC. Moreover, MOUKPC shows better adhesion and hence contains negligibly small amount of voids [Figure 7(d)] for which the WU is lessened in this sample, as compared to the others.

Degradation of Mechanical Properties

The deterioration of TS of the samples under artificial accelerated weathering condition has been observed for all samples at various time durations, as shown in Figure 12. A comparison of TS degradation between the data of 0 and 1800 h for RPP, RKPC, MRKPC, and MOUKPC are 10, 35, 30, and 17%, respectively. Thus, the use of treated fiber and coupling agent

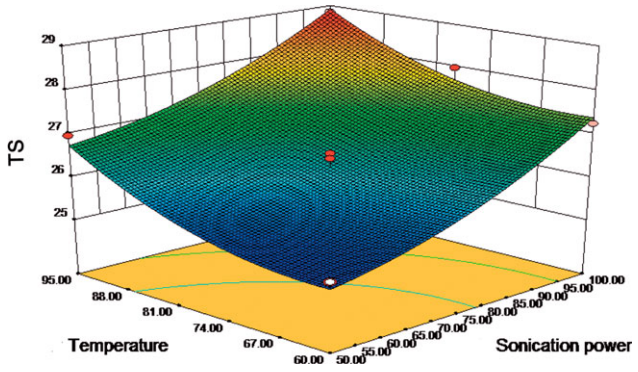

Figure 15. A 3-D plot of the response as a function of temperature and sonication power. [Color figure can be viewed in the online issue, which is available at wileyonlinelibrary.com.]

results in durable composites. The reduction of TS for RPP, RKPC, MRKPC, and MOUKPC between the data before WU (BWU) and after WU (AWU), as shown in Figure 13, is observed to be 0, 13, 12, and 6%, showing that inclusion of MAPP retards the degradation process.

Optimization of Parameters by RSM

Using the suggestive parameters of SP and T by the DES, the composites prepared in this study show the experimental TS values which are included in Table V. With these values DES provides further parameters. From these data, the plots of predicted versus actual value (Figure 14), which lies very close to the straight line, suggest that the model is significant. The 3-D plot (Figure 15) of TS as a function of both temperature and sonication power as well as the interaction plot (Figure 16) of TS versus sonication power at various temperatures clearly demonstrate that increasing of both parameters increases the TS. The best set of treatment conditions, as suggested by the software, are SP = 99.96% and $T = 94.46$°C, which give rise to the highest TS value of 28.86 MPa. This result is in a reasonably good agreement with our experimentally observed values of SP = 100%, T = 95°C, showing TS = 28.84 MPa.

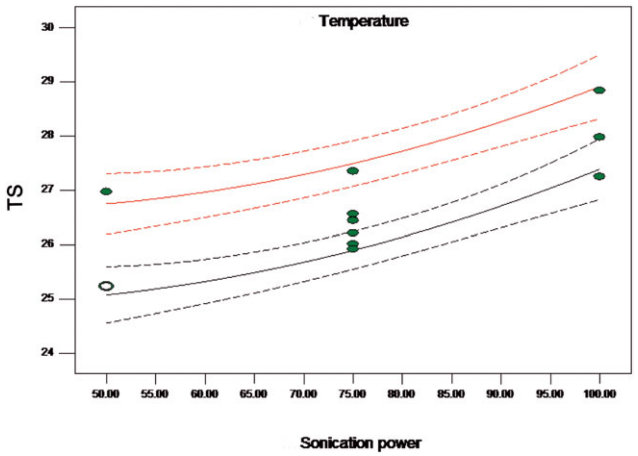

Figure 16. Interaction graph of the response as a function of temperature and sonication power. [Color figure can be viewed in the online issue, which is available at wileyonlinelibrary.com.]

CONCLUSIONS

ULS treatment at various temperatures removes lignin, pectin, hemicelluloses, and other surface impurities, as verified by FTIR analysis. The observed optimal treatment parameters are temperature of ~ 95°C and sonication power of ~ 100% with respect to the maximum TS (28.84 MPa) and TM (1035 MPa) values. A strong adhesion between fibers and matrix in the composites has been achieved with treated fiber and coupling agent. Treated fiber in the presence of coupling enhances the crystallinity and the thermal stability of the composites. A comparative study regarding moisture absorption and weather conditioning of the composites based on treated fiber in the presence of coupling agent reveals less absorbed water and more stability in the accelerated weathering condition as compared to the composites based on raw fiber and without uncoupling agent. Most importantly, the treatment parameters were verified by RSM, which shows the values close agreement to those observed in our experiments.

ACKNOWLEDGMENTS

Authors would like to acknowledge the Ministry of Higher education, Malaysia for providing financial support through FRGS (RDU120106) for this project.

REFERENCES

1. Satyanarayana, K. G.; Sukumaran, K.; Mukherjee, P. S.; Pavithran, C.; Pillai, S. G. K. *Cem. Concr. Compos.* **1990,** *12*, 117.
2. Xie, Y.; Hill, C. A. S.; Xiao, Z.; Militz, H.; Mai, C. *Compos. A* **2010,** *41*, 806.
3. Kabir, M. M.; Wang, H.; Lau, K. T.; Cardona, F. *Compos. B* **2012,** *43*, 2883.
4. Nam, T. H.; Ogihara, S.; Tung, N. H.; Kobayashi, S. *Compos. B* **2011,** *42*, 1648.
5. Gomes, A.; Matsuo, T.; Goda, K.; Ohgi, J. *Compos. A* **2007,** 38, 1811.
6. Gassan, J.; Bledzki, A. K. *Compos. Sci. Technol.* **1999,** *59*, 1303.
7. Asumani, O. M. L.; Reid, R. G.; Paskaramoorthy, R. *Compos. A* **2012,** *43*, 1431.
8. Mylsamy, K.; Rajendran, I. *Mater. Des.* **2011,** *32*, 4629.
9. Kim, H. S.; Lee, B. H.; Choi, S. W.; Kim, S.; Kim, H. *J. Compos. A* **2007,** *38*, 1473.
10. Didenko, Y. T.; McNamara, W. B.; Suslick, K. S. *J. Am. Chem. Soc.* **1999,** *121*, 5817.
11. Liu, L.; Huang, Y. D.; Zhang, Z.Q.; Jiang, Z. X.; Wu, L. N. *Appl. Surf. Sci.* **2008,** *254*, 2594.
12. Wei, L.; Jinquan, Y.; Shouxin, L. *Ultrasound Sonochem.* **2012,** *19*, 479.
13. Karunanithy, C.; Muthukumarappan, K. *Ind. Crops Prod.* **2011,** *33*, 188.
14. Corradini, E.; Ito, E. N.; Marconcini, J. M.; Rios, C. T.; Agnelli, J. A. M.; Mattoso, L. H. C. *Polym. Test.* **2009,** *28*, 183.
15. Lei, Y.; Wu, Q.; Yao, F.; Xu, Y. *Compos. A* **2007,** *38*, 1664.
16. Broido, A. *J. Polym. Sci. Part A-2: Polym. Phys.* **1969,** *7*, 1761.
17. Paul, A.; Joseph, K.; Thomas, S. *Compos. Sci. Technol.* **1997,** *57*, 67.
18. Gañán, P.; Zulunga, R.; Restrepo, A.; Labidi, J.; Mondragon, I. *Bioresour. Technol.* **2008,** *99*, 486.
19. Haque, M. M.; Hasan, M.; Islam, M. S.; Ali, M. E. *Bioresour. Technol.* **2009,** *100*, 4903.
20. Suradi, S. S.; Younus, R. M.; Beg, M. D. H. *J. Compos. Mater.* **2010,** *45*, 1853.
21. Katsoulotos, G.; Pappa, G.; Tarantili, P. A.; Magoulas, K. *Polym. Eng. Sci.*, **2008,** *48*, 902.
22. Alvarez, V. A.; Vázquez A. *Polym. Degrad. Stab.* **2004,** *84*, 13.
23. Garcia, M.; van Vliet, G.; Jain, S.; Schrauwen, B. A. G.; Sarkissov, A.; van Zyl, W. E.; Boukamp, B. *Adv. Mater. Sci.* **2004,** *6*, 169.
24. Qin, L.; Qiu, J.; Liu, M.; Ding, S.; Shao, L.; Lü, S.; Zhang, G.; Zhao, Y.; Fu, X. *Chem. Eng. J.*, **2011,** *166*, 772.
25. Marcovich, N. E.; Villar, M. A. *J. Appl. Polym. Sci.*, **2003,** *90*, 2775.